8th International Conference
on
Wind Turbine Noise
Lisbon – 12th to 14th June 2019

Scales of turbulence on a wind turbine leading–edge

Ronan Serré
Vestas Design Center, R. Lionesa 31, 4465–332 Leça do Balio, Portugal

Kristian Balschmidt Godsk
Vestas Wind Systems A/S, Hedeager 42, Aarhus, 8200, Denmark

Tomas Vronsky
Vestas Technology UK Ltd, Stag Lane, Newport, Isle of Wight, PO30 5TR, United–Kingdom

Summary

Turbulence intensity and integral length scale are two parameters driving leading–edge noise radiation. In the wind turbine industry, these quantities are generally estimated from empirical relations for atmospheric boundary layers but the turbulence actually experienced by the leading–edge during the blade rotation in wind turbine applications is believed to be more relevant to characterise leading–edge noise and to significantly differs from atmospheric boundary layer turbulence. This contribution investigates the influence of turbulence intensity and integral length scale estimations on wind turbine leading-edge noise prediction and compare the turbulence properties in the atmospheric boundary layer with what can be typically found on a wind turbine leading–edge. A more representative scaling of the inflow turbulence is proposed.

1. Introduction

Aerodynamic noise from a wind turbine is seen to originates predominantly from the trailing–edge as a result of the scattering of the boundary layer pressure waves and from the leading–edge as a response to the incoming turbulence [1]. Trailing–edge noise being gradually reduced, the contribution of the leading–edge noise is gaining importance and in addition, being in the low frequency region,

survives on higher propagation distances, being less affected by air absorption [2]. Leading–edge noise modeling principally relies on the turbulence intensity and integral length scale of the incoming disturbances [3]. In the wind turbine industry, these quantities are generally estimated from empirical relations for atmospheric boundary layers [4]. Coupled with empirical models for leading-edge noise, the numerical predictions are generally found in close agreements with field test measurements. But such agreements may only be a consequence of the empirical models for leading–edge noise being in fact specifically calibrated for the empirical estimation of the turbulence scales in the boundary layer and this might not hold for analytical models for leading–edge noise as the turbulence that needs to be specified is relative to the chordwise component of the inflow velocity [3]. Tian and Cotté [1] used Amiet theory for leading–edge noise modeling coupled with empirical atmospheric boundary layer turbulence but with specific constants to adapt the estimated turbulence. And a wide variety is found in the turbulence intensity and integral length scale values generally adopted [1, 4, 5], indicating that no clear consensus exists in the community. Two remarks follow: *i)* if constants are freely modifiable to determine turbulence properties in atmospheric boundary layers might lead to a non–homogeneous use of the noise models and to inconsistant results among the community and *ii)* the turbulence characterics of the atmospheric boundary layer might not be the most relevant for leading-edge noise prediction in wind turbine application. The early work on wind turbine noise prediction of Glegg et al. [6] initiated a discussion on the relevance of the integral length scale in atmospheric boundary layer for leading–edge noise modeling of wind turbines. In this study, the orders of magnitude were judged too high and it was proposed to set the integral length scale as the blade chord. However, the relevance of these conclusions are also questionnable as the analysis was based on a wind turbine with a rotor diameter of 20 m, that is, quite different from the present generation of wind turbines. The pioneering theoretical work of Amiet [3] specificies that leading–edge noise radiation is directly dependant on the turbulence impinging the leading–edge, in the chordwise direction. It should then be preferable to avoid relying on empirical relations suited for atmospheric boundary layers and instead rely as far as possible on inflow aerodynamic data. This contribution presents an empirical and an anlytical model for leading–edge noise prediction and the impact of the turbulence properties through three empirical formulations for turbulence estimation compared with direct measurement of the turbulence intensity and integral length in the chordwise direction of a wind turbine leading–edge from field test measurements of the DanAero campaign [5, 7] and numerical modeling with an in–house numerical tool.

2. Numerical tool

2.1. Description

The numerical tool, hereinafter referred to as VTS, consists in one aeroelastic and one aeroacoustic tool. The aeroelastic tool models the dynamic behavior of horizontal axis wind turbines operating in specified wind conditions, such as simulated turbulent wind and wind shear [8]. The program runs in the time-domain producing time-series of loads and deflections. Aerodynamics is calculated using the BEM method with additional modeling to account for unsteadiness, dynamic wake, dynamic stall and yaw and/or tilt conditions. The aeroacoustic tool uses the aerodynamic inflow prediction to predict trailing–edge and leading–edge noise of isolated aerofoils or wind turbine blades from empirical [4, 9] or analytical models [10], according to the IEC standard [11]. The attenuation of the

acoustic energy in atmospheric propagation by air absorption is modeled following the guidelines discussed by Salomons [2]. This contribution aims at addressing the leading–edge noise modeling but in field test measurements of wind turbine noise, the different contributions cannot be isolated. For this reason, when numerical predictions are compared to field test measurements of wind turbine noise, empirical modeling of the trailing–edge noise [9], referred to as "TBL–TE", is simply added for information. Only leading–edge noise empirical and analytical models are presented below.

2.2. Empirical modeling for leading–edge noise

The expression for the sound pressure level SPL in the empirical model reads as [4, 12]:

$$SPL = 10\ \log_{10}\left[\overline{D}_l \rho_0^2 c_0^2 \Lambda_{uu} \frac{L}{r_{obs}^2} M^3 T_i^2 \hat{k}^3 \left(1+\hat{k}^2\right)^{-7/3}\right] + 10\ \log_{10}\left(\frac{K_c}{1+K_c}\right) + 58.4 \tag{1}$$

with ρ_0 as the uniform medium density, c_0 the speed of sound, r_{obs} the observer distance, $M = U_0/c_0$ the Mach number, U_0 being the mean inflow velocity and L the aerofoil or blade element span length. The inflow turbulence parameters, T_i and Λ_{uu} are in this context defined as the turbulence intensity and integral length scale of the longitudinal velocity fluctuations in the atmospheric boundary layer, estimated by an empirical model described by Counihan [13], although it will hereinafter referred to as "Zhu" model. The model uses a constant defined as the surface roughness that is required to be ajusted by the user. Throughout this contribution, when referring to the Zhu model, the surface roughness is set as 0.01 m following Zhu et al. [4]. The function $\overline{D}_l$ is a low frequency directivity function as expressed by Brooks et al. [9]. with $\hat{k} = \pi f C/U_0$ a normalised wavenumber (with f the frequency and C the aerofoil or blade element chord length) and K_c a low frequency correction factor.

$$K_c = \frac{10M\hat{k}^2/\beta^2}{\left(2\pi\hat{k}/\beta^2\right) + \left(1+2.4\hat{k}/\beta^2\right)^{-1}} \tag{2}$$

with $\beta^2 = 1 - M^2$, the Prandtl–Glauert compressibility coefficient.

2.3. Analytical modeling for leading–edge noise

The expression for the instantaneous power spectrum density of the acoustic pressure S_{pp} in the analytical model, reads as [10]:

$$S_{pp}\left(\overrightarrow{x},\omega\right) = \left(\frac{\rho_0 \omega x_3}{2c_0 S_0^2}\right)^2 \pi U_0 \frac{L}{2} \phi_{ww}\left(k_1,k_2\right) \left|\mathcal{L}_{TI}\left(x_1,k_1,k_2\right)\right|^2 \tag{3}$$

with $\omega = 2\pi f$ the pulsation, $\overrightarrow{x}$ the observer coordinates in the frame of reference expressed in reference [9] (x_1 refers to the chordline, x_2 to the spanline and x_3 to the normal direction). The function S_0 accounts for the convective observer distance $S_0^2 = x_1^2 + \beta^2\left(x_2^2 + x_3^2\right)$. The function $\mathcal{L}_{TI}$ is an aeroacoustic transfer function described in details in reference [10]. The function ϕ_{ww} is the two–dimensionnal wavenumber spectrum of the upwash velocity fluctuations and can be estimated by Kármán model [3]:

$$\phi_{ww}\left(k_1,k_2\right) = \frac{3}{4\pi} T_i U_0 \Lambda_{uu}^2 \frac{\Lambda_{uu}^2\left(k_1^2+k_2^2\right)}{\left[1+\Lambda_{uu}^2\left(k_1^2+k_2^2\right)\right]^{5/2}} \tag{4}$$

with k_1 and k_2 the wavenumbers in the chordwise and spanwise directions, respectively. It relies on the turbulence intensity T_i and the integral length scale Λ_{uu}, here, specifically based on the chordwise velocity component [3].

2.4. Aerofoil noise assessment

Empirical and analytical modeling are first applied to estimate leading–edge noise on a NACA–0012 isolated aerofoil in a wind tunnel to replicate a study published by Paterson and Amiet [14] for a range of Reynolds number based on the chord length varying from 0.5×10^6 to 2.5×10^6 (corresponding to Mach numbers ranging from 0.12 to 0.5), at zero degree angle of attack. The turbulence intensity and integral length scale are imposed as 4 % and 0.03 m, respectively [14]. Figure 1 presents the sound pressure level spectra SPL, in dB. The empirical modeling (dashed lines) underestimates significantly the sound pressure levels at all frequencies. The analytical modeling (solid lines) is in better agreement with the measurements (symbols), some singularities notwithstanding. In the high frequency region however, the sound pressure levels tend to be overestimated.

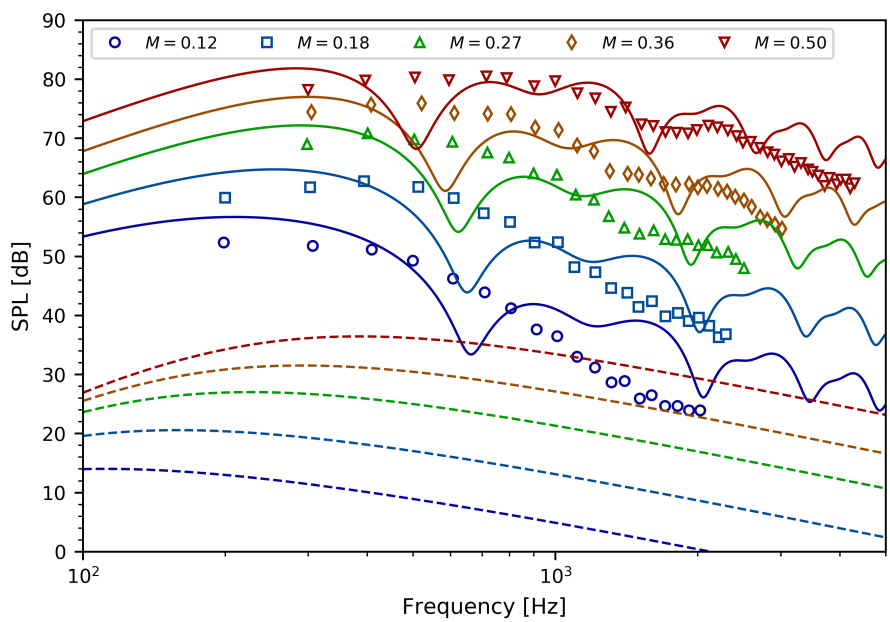

Fig. 1 Aerofoil noise prediction on a NACA–0012. Measurements from Paterson and Amiet [14] (symbols), empirical modeling (dashed lines) and analytical modeling (solid lines). The colours indicate the Mach number.

2.5. Wind turbine noise assessment

Empirical and analytical modeling are then applied to estimate the acoustic power radiated by a representative wind turbine and compare with field test measurements. The Vestas V80 is a 2 MW horizontal axis wind turbine with hub height of 60 m and a 40 m blade span. Here, the turbulence intensity and integral length scale are estimated as proposed in reference [4], in the empirical modeling framework, in the context of atmospheric boundary layer. The total acoustic power L_wA is depicted in figure 2 for a range of wind speed at hub height V_{hub} and the corresponding sound power level

spectrum L_wAf at peak noise ($V_{hub} = 11$ m/s) in figure 3. An estimation of trailing–edge noise from empirical modeling [9] is added to the figure, to account for the fact that the contributions from the field test measurement cannot be isolated. In figure 2, the empirical modeling gives a more realistic prediction, slightly lower than trailing–edge noise noise and measurements while the prediction from analytical modeling is clearly overestimated. The same observation is made in the frequency domain (figure 3) with the low frequency region being clearly overestimated by the analytical modeling.

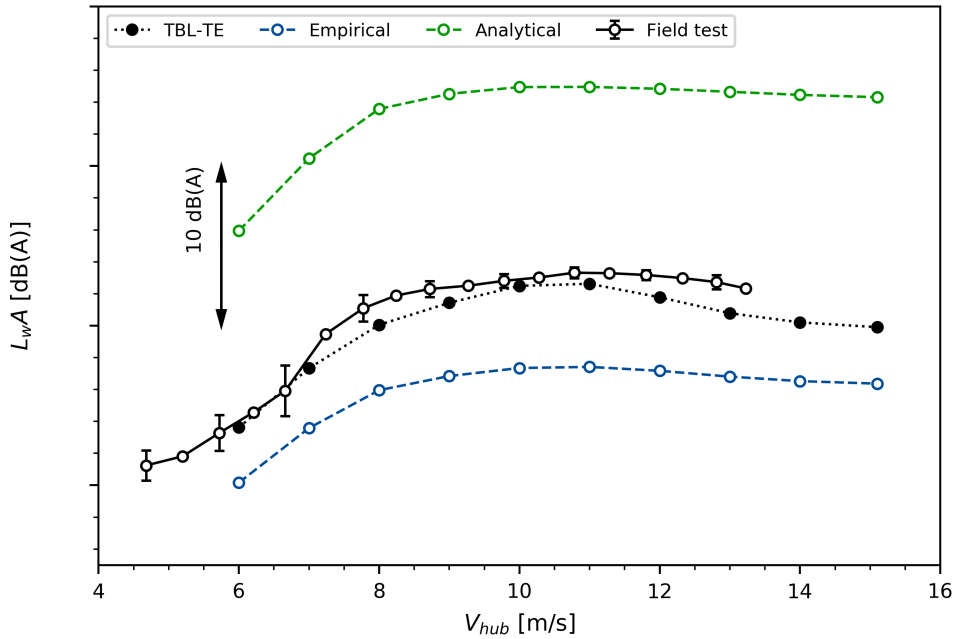

Fig. 2 Acoustic power. Atmospheric boundary layer turbulence. V80 wind turbine.

2.6. Preliminary discussion

For the leading–edge noise prediction of an isolated aerofoil, the analytical modeling is in better agreement with the measurements than the empirical modeling. However, for the leading–edge noise prediction of a wind turbine, the empirical modeling provides a better agreement. In the context of inflow turbulence, it is observed that the analytical modeling provides a realistic prediction when the inflow turbulence is prescribed but fails when the inflow turbulence is estimated by an atmospheric boundary layer model. In other words, the empirical modeling might give satisfaction only as a consequence of being calibrated to a specific inflow turbulence and this specific inflow turbulence might not be relevant to describe the actual inflow turbulence experienced by a wind turbine leading–edge, thus explaining the inaccuracy of the analytical modeling on wind turbine noise. Consequently, there is a need to assess the typical values for turbulence actually impinging a wind turbine leading and propose new inflow turbulence modeling in order to develop the use of analytical modeling for leading–edge noise prediction in wind turbine applications.

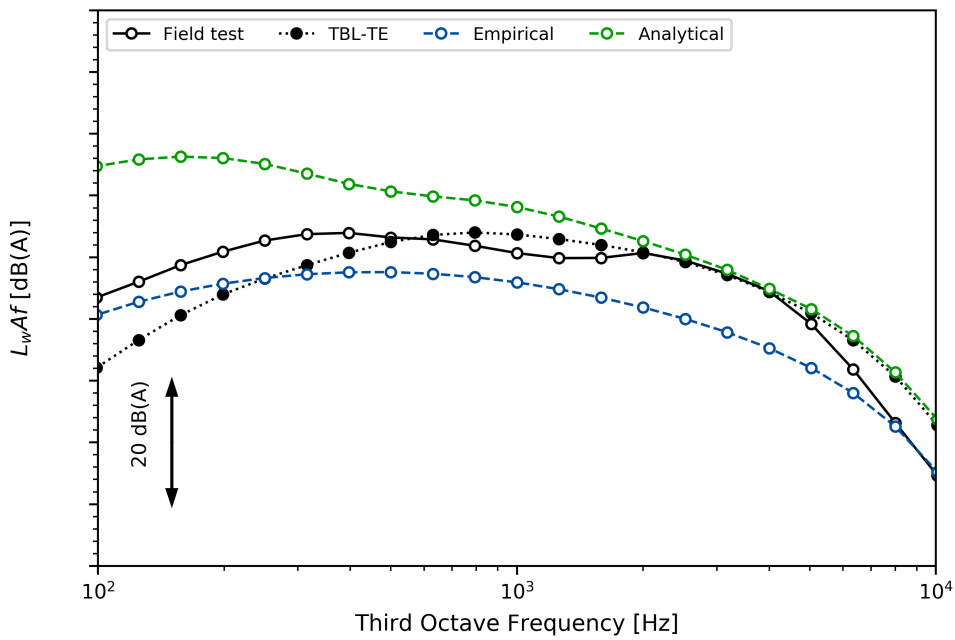

Fig. 3 Acoustic power spectra. Atmospheric boundary layer turbulence. V80 wind turbine. $V_{hub} = 11$ m/s.

3. Direct estimation of the inflow turbulence

Aerodynamic data from a field test measurement campaign, referred to as DanAero [7], and VTS are used to estimate the typical values for the turbulence actually impinging a wind turbine leading–edge. In the DanAero experiment, aerodynamic inflow conditions were measured for several spanwise locations on a 2.3 MW NM80 horizontal axis wind turbine with hub height of 57 m and a 40 m blade span, for a wind speed measured at hub height of approximately 6.2 m/s. The objective is to have a first estimation of the order of magnitude of the inflow turbulence characteristics from two different sources, through field test measurements and aerodynamic modeling to assess how far it might deviate from the inflow turbulence values estimated with an empirical atmospheric boundary layer approach. The Vestas wind turbine selected for VTS computations, the V80, is relatively similar to the wind turbine instrumentalised in the DanAero experiment. For VTS computations, the wind shear $V(z)$ is specified to fit the measured wind velocity profile, from IEC standard [8]:

$$V(z) = V_{hub} \times \left(\frac{z}{z_{hub}}\right)^{\alpha} \tag{5}$$

with z the vertical height above ground and z_{hub} the hub height. The exponent α determines the velocity profile and is imposed as $\alpha = 0.08$. The wind shear velocity profiles, as recommended by the IEC standard, measured from VTS and in the DanAero experiment are shown in figure 4. The atmospheric conditions are then consistent between the field test measurements and the numerical modeling. In the present contribution, one sensor location is used, at 80 % of the blade span ($r/R = 0.8$) to estimate the turbulence intensity and integral length scale of the chordwise velocity component and compared with the same estimation from VTS on the V80 (at the same relative spanwise location). The chordwise component of the inflow velocity u is retrieved from the DanAero

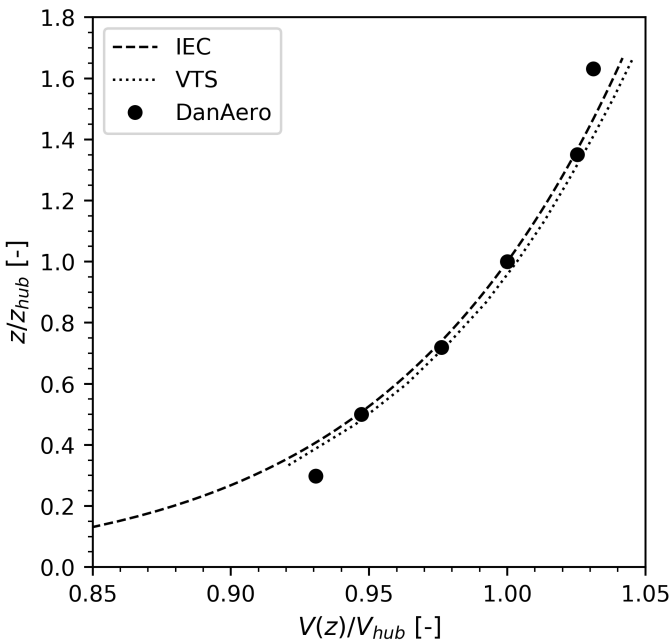

Fig. 4 Wind shear velocity profiles as specified by IEC standard, imposed in VTS and measured in the DanAero experiment.

experiment (with a sampling frequency of 35 Hz) and from VTS (with a sampling frequency of 25 Hz). In both cases, the acquisition time is 600 s (10 minutes). The velocity signals are considered made of a mean part (phase averaged) and a fluctuating part as $u = \overline{u} + u'$ with the overline denoting the mean part and the prime the fluctuating part. The turbulence intensity is defined as [15]

$$T_i = \frac{\sigma_{u'}}{\overline{u}} \tag{6}$$

with $\sigma_{u'}$ the standard deviation of the chordwise velocity fluctuations. The integral length scale is defined as the length scale over which the most energetic eddies are correlated. Following the estimation procedure from Thacker et al. [16], the chordwise velocity autocorrelation function is defined as

$$R_{uu}(\tau) = \frac{\overline{u'(t) \cdot u'(t+\tau)}}{\sqrt{\overline{u'(t)^2} \cdot \overline{u'(t+\tau)^2}}} \tag{7}$$

where τ is a variable time step in the signal history. The integral time scale follows as the time integration until the first zero–crossing of the autocorrelation:

$$t_{uu} = \int_0^\infty R_{uu}(\tau)\, \mathrm{d}\tau \tag{8}$$

then leading to the integral length scale definition as

$$\Lambda_{uu} = \overline{u} \times t_{uu} \tag{9}$$

The autocorrelation function and the corresponding integral length scale are estimated every 1 s from 100 s to 500 s in the available time signals. The autocorrelation functions estimated from DanAero and

VTS are presented in figure 5, averaged over the time blocks, with the variable time step τ normalised by the corresponding rotation period T. The standard deviation is relatively low, indicating that there might be no significant changes in the integral length scale with the blade azimuthal position in the rotation cycle.

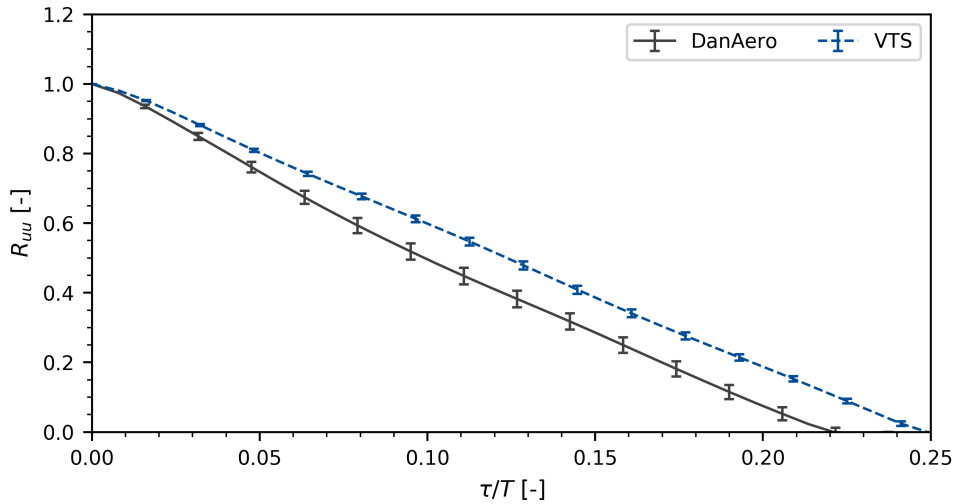

Fig. 5 Autocorrelation functions estimated from measurements in the DanAero experiment and VTS. The time is normalised by the rotation period.

4. Comparison with empirical estimations for turbulence

The values for the turbulence intensity and integral length scale directly estimated from the DanAero experiment and VTS are compared to values estimated from three empirical formulations for atmospheric boundary layers, applied with the same conditions used in VTS, on the V80 wind turbine. The three empirical atmospheric boundary layer models are: *i)* an aforementioned model referred to as "Zhu" from Zhu et al. [4], *ii)* a model referred to as "Tian" from Tian and Cotté [1] and *iii)* a model referred to as "Bertagnolio", following an empirical relation described in reference [5]. The same time discretisation by blocks of 1 s between 100 s and 500 s previously used is also applied to the empirical formulations in order to see the evolution of the inflow turbulence with time and in particular, to notice any effect of the blade azimuthal position in the rotation cycle. Figure 6 and figure 7 respectively present the turbulence intensity and the integral length scale from the DanAero experiment, VTS and the three empirical formulations along one rotation period. Regarding the turbulence intensity (figure 6), only the Zhu formulation predicts an evolution with the blade azimuthal position, although relatively small. The empirical formulations predict a turbulence intensity significantly higher than the direct estimation from the DanAero experiment and VTS (between 10 % and 15 % for the empirical estimations and around 2 % for the direct estimations). Regarding the integral length scale (figure 7), the three empirical formulations predict an evolution with the blade azimuthal position and here, relatively significant. However, from the direct estimations, the integral length scale does not seem to be affected by the blade azimuthal position. The striking fact is however the order of magnitude of the different length scale estimations: a few dozen meters from the direct estimations and a few hundred meters from the empirical estimations. The mean values (and the standard deviation associated with

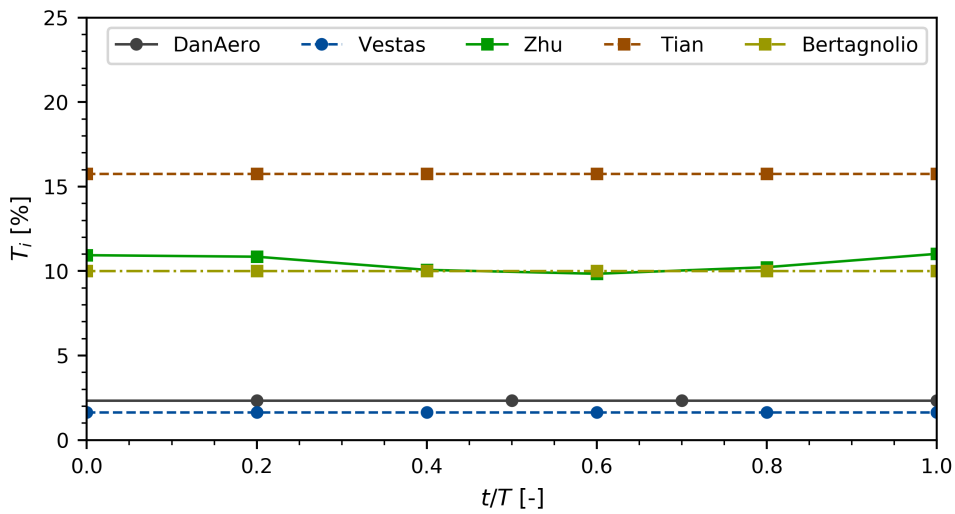

Fig. 6 Turbulence intensities. The time is normalised by the rotation period.

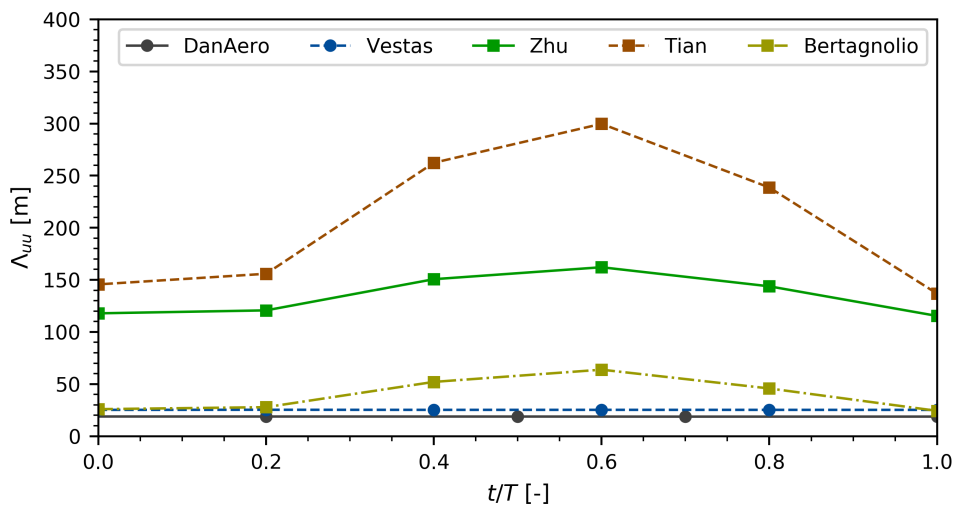

Fig. 7 Turbulence integral length scales. The time is normalised by the rotation period.

the integral length scale) are summarized in table 1.

	DanAero	VTS	Zhu	Tian	Bertagnolio
T_i [%]	2.3	1.6	10.4	15.7	10.0
Λ_{uu} [m]	18.1 ± 0.7	25.0 ± 0.3	139.3 ± 17.4	221.4 ± 61.1	43.3 ± 14.6

Table 1 Mean values with standard deviation for the turbulence intensity T_i and integral length scale Λ_{uu} estimations.

5. Influence of the turbulence inflow conditions on noise modeling

The impact of the different inflow turbulence estimations on the leading–edge noise prediction is now discussed. The total acoustic power is depicted in figure 8 and the corresponding sound power level spectrum at peak noise ($V_{hub} = 11$ m/s) in figure 9 from empirical modeling. An estimation of trailing–edge noise from empirical modeling [9] is added to the figure. In both figures it is observed that if the direct estimations for the inflow turbulence is used, the empirical leading–edge noise modeling underestimates the field test measurements but manages to yield relative agreements with empirical inflow turbulence estimations. In the context of analytical modeling, Roger and Moreau [10]

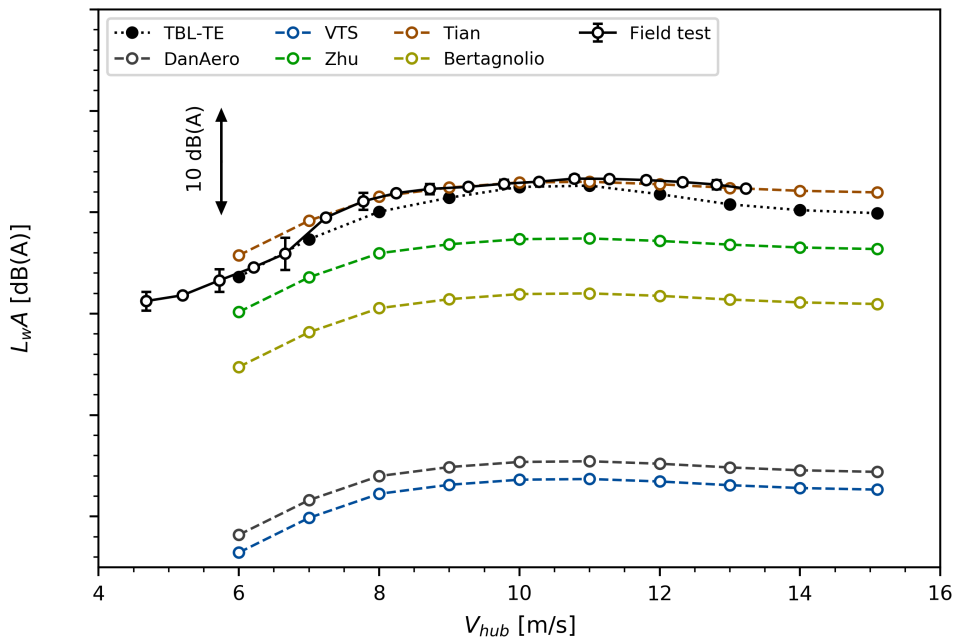

Fig. 8 Acoustic power. Empirical modeling. V80 wind turbine.

stated that the velocity fluctuation spectrum in the mid–span plane $\phi_{ww}(k_1, 0)$ scales as the upwash velocity power spectral density $S_{ww}(\omega)$. Figure 10 presents this scaling with the velocity fluctuation spectrum in the mid–span plane $\phi_{ww}(k_1, 0)$ estimated with the Kármán model for the different inflow turbulence estimations. The low frequency sampling notwithstanding, the velocity spectrum is better captured with the direct estimations of the inflow turbulence than with the empirical estimations and specially the peak frequency. The empirical estimations are expected to overpredict the leading–edge noise prediction. The total acoustic power is depicted in figure 11 and the corresponding sound power level spectrum at peak noise ($V_{hub} = 11$ m/s) in figure 12 from analytical modeling. An estimation of trailing–edge noise from empirical modeling [9] is added to the figure. Here, the opposite observation is made. Analytical modeling with empirical inflow turbulence overpredicts the leading–edge noise but gives relative agreement with the direct inflow turbulence estimations.

6. Towards a scaling of the inflow turbulence

Evidences suggest that the empirical estimation of the inflow turbulence from atmospheric boundary layer models do not account for the inflow turbulence actually experienced by a wind turbine

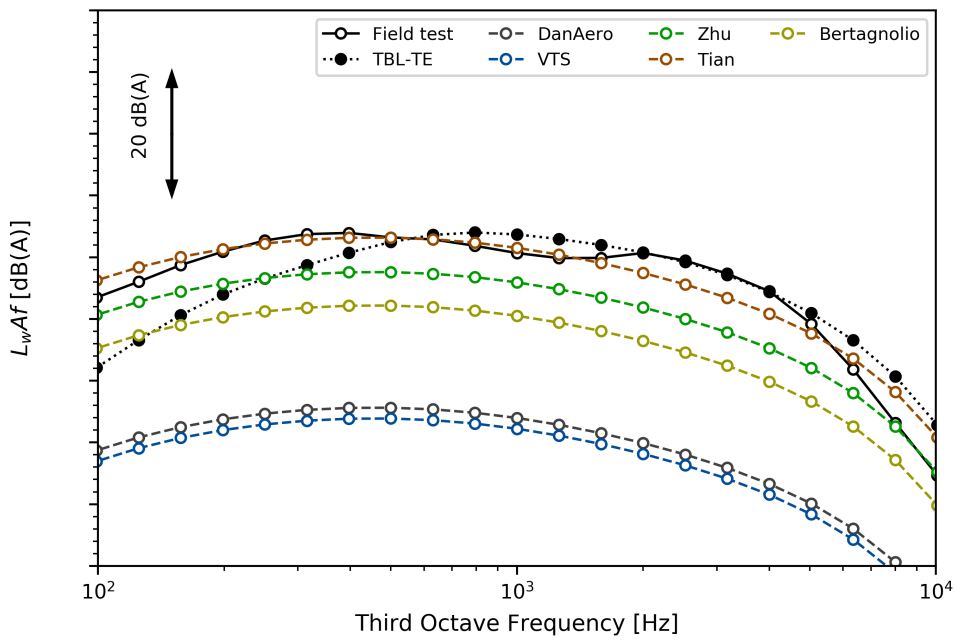

Fig. 9 Acoustic power spectra. Empirical modeling. V80 wind turbine. $V_{hub} = 11$ **m/s.**

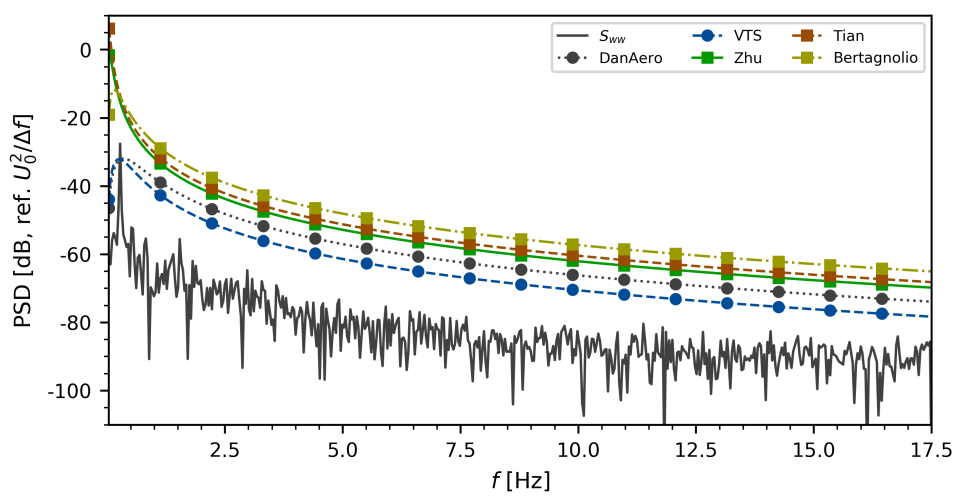

Fig. 10 Velocity spectrum scaling. The amplitudes are scaled with the mean inflow speed U_0 **and the frequency resolution** Δf**.**

leading–edge that is required for analytical leading–edge noise modeling. Instead, the turbulence properties estimated from the numerical tool are in fact similar to what can be estimated from field test measurements. From the same numerical tool VTS applied on a range of wind turbines, for several wind speeds at hub height, a more representative scaling can be proposed. Figure 13 presents the data reduction of turbulence intensities estimated from VTS for a range of wind turbines and wind speeds at hub height. A collapse of the data can be observed that leads to propose a scaling in the form of equation 10, with r as the radial location.

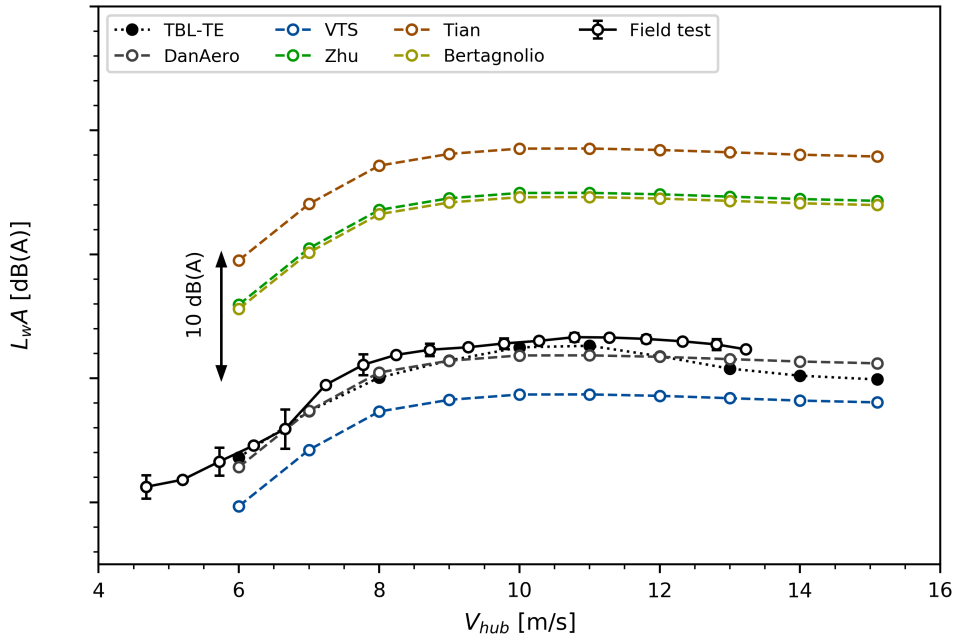

Fig. 11 Acoustic power. Analytical modeling. V80 wind turbine.

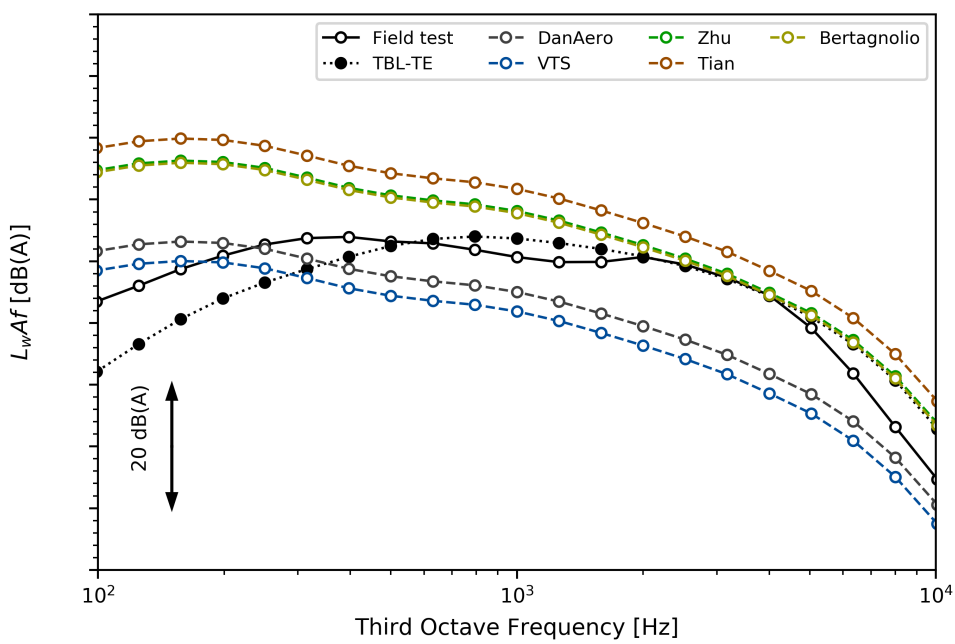

Fig. 12 Acoustic power spectra. Analytical modeling. V80 wind turbine. $V_{hub} = 11$ **m/s.**

$$T_i = A\left(\frac{V_{hub} \times T}{r}\right)^B + C \tag{10}$$

The turbulence intensity is expressed in percentage. Figure 13 presents the data reduction of integral length scales estimated from VTS for a range of wind turbines and wind speeds at hub height. A

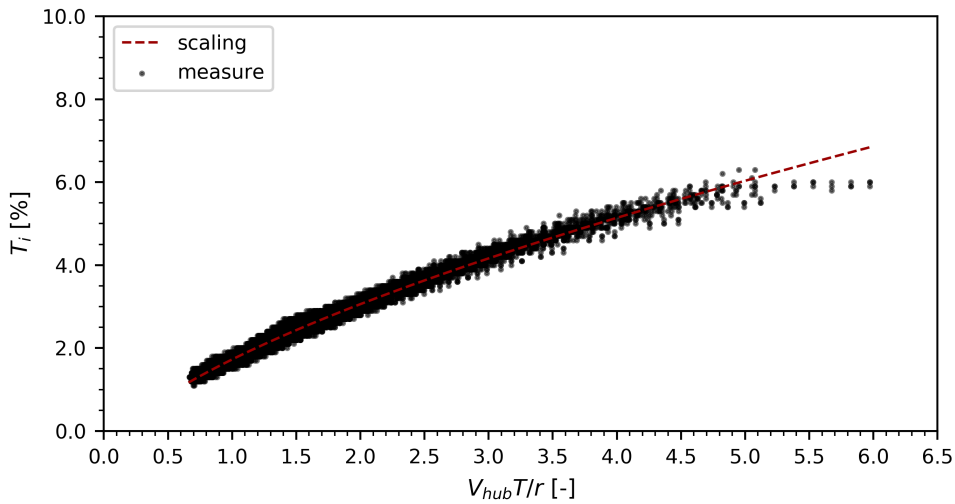

Fig. 13 Data reduction of turbulence intensities estimated from VTS.

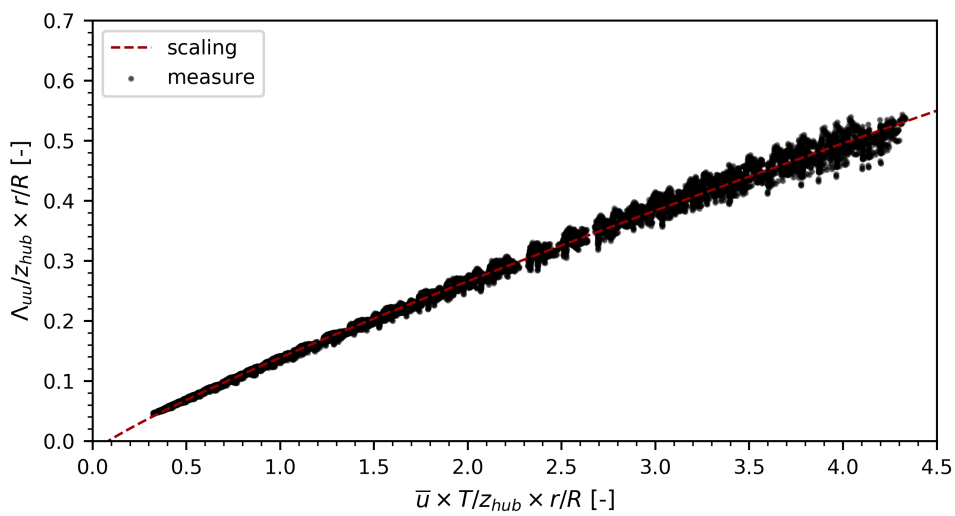

Fig. 14 Data reduction of integral length scales estimated from VTS.

relative collapse of the data can be observed that leads to propose a scaling in the form of equation 11, with R, the blade tip radius. The coefficients, found with a non–linear least squares method [17], are summarized in table 2.

$$\frac{\Lambda_{uu}}{z_{hub}}\frac{r}{R} = A\left(\frac{\overline{u}\times T}{Z_{hub}}\frac{r}{R}\right)^{B} + C \tag{11}$$

If the scaling provides a satisfying agreement with the direct estimation for the turbulence intensity (figure 13) as a consequence of a better collapse of the normalised data, the scaling of the integral length scale however (figure 14) tends to diverge towards the tip ($r/R \sim 1$). This suggests to view the proposed scalings as preliminary results. Figures 15 and 16 show the acoustic power prediction (of both trailing–edge and leading–edge noise combined) and the corresponding frequency content (at $V_{hub} = 11$ m/s) from the empirical modeling with empirical estimation of the inflow turbulence

	A	B	C
Scaling coefficients for T_i	2.376	0.643	−0.651
Scaling coefficients for Λ_{uu}	0.158	0.853	−0.020

Table 2 Scaling coefficients for the inflow turbulence.

and the analytical modeling with the scaling of the inflow turbulence. When the scaling is applied with the analytical leading–edge noise modeling, the agreement is satisfying at low wind speed but rapidly starts overpredicting the total acoustic power at higher wind speeds (figure 15). To assess the source of the discrepancies at higher wind speeds, a more thorough analysis needs to be carried with experimental measurements for several wind speeds at hub height. Then, the ability of the numerical tool to represent turbulence levels for a range of wind speeds at hub height could be validated.

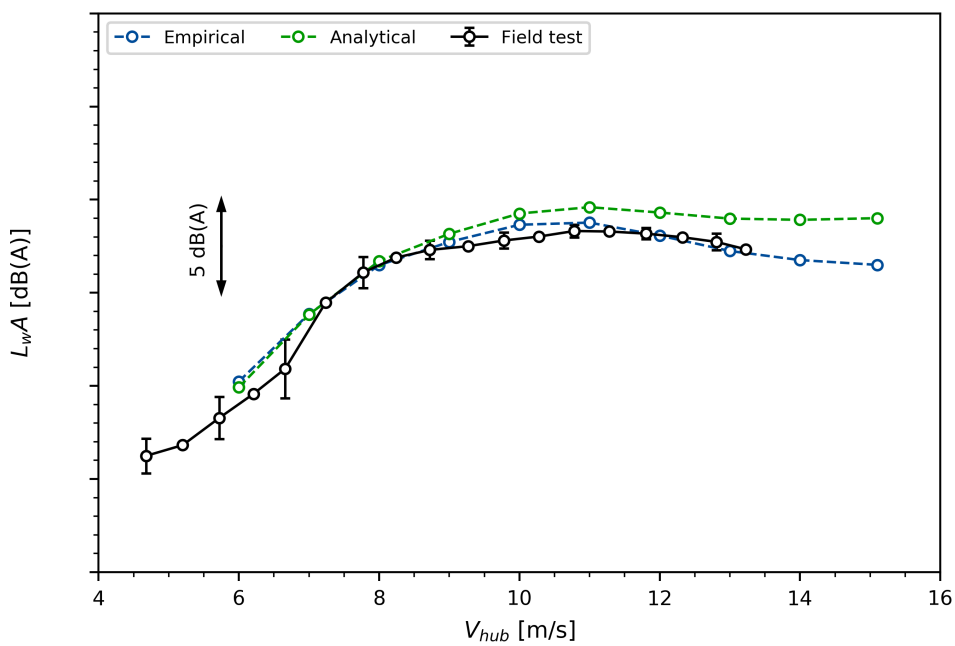

Fig. 15 Total acoustic power. Empirical modeling with atmospheric turbulence and analytical modeling with inflow turbulence scaling. V80 wind turbine.

7. Conclusion

The description of the inflow turbulence, in terms of turbulence intensity and integral length scale is crucial for leading–edge noise prediction. From the materials presented in this contribution, its estimation from empirical formulations of atmospheric boundary layer is believed to be valid only for empirical leading–edge noise modeling that are in fact specifically calibrated for these levels of turbulence. However, when using analytical leading–edge noise modeling, the empirical turbulence estimations fails and knowledge of the turbulence based on the chordwise velocity component at the leading–edge is needed. Turbulence intensity and integral length scale impinging a wind turbine

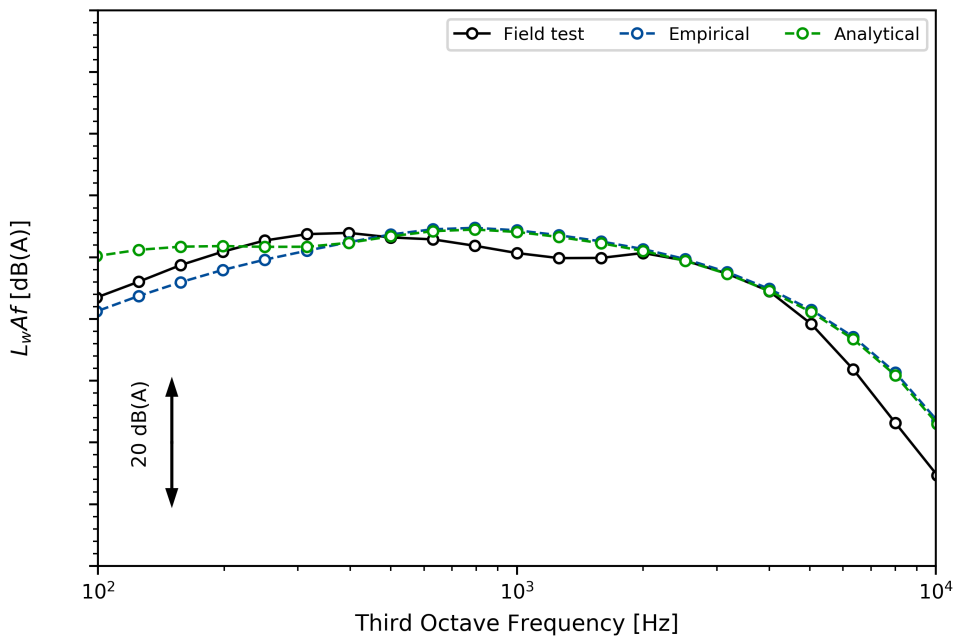

Fig. 16 Total acoustic power spectra. Empirical modeling with atmospheric turbulence and analytical modeling with inflow turbulence scaling. V80 wind turbine. $V_{hub} = 11$ **m/s.**

leading–edge have been measured and have been shown to differ significantly from the empirical estimations. Direct estimations show lower turbulence intensity and lower integral length scale than what can be estimated from the empirical formulations. The direct estimations also indicate relatively constant turbulence levels during a rotation period and that is also in contradiction with the empirical estimations. This contribution has shown that, with analytical leading–edge noise modeling, the leading–edge turbulence can be estimated from a low–order numerical tool to give representative noise predictions but that should not lead to disregard the importance of atmospheric boundary layer turbulence models but instead should lead to re-organise the methodolgy. The atmospheric boundary layer turbulence modeling should be used in the aerodynamic part of the numerical tool to yield estimation of the chordwise velocity at the leading–edge of the blades and once that is known, the turbulence intensity and integral length based on the chordwise component could be directly estimated and used as input for the analytical leading–edge noise modeling.

References

[1] Y. Tian and B. Cotté. Wind turbine nosie modeling based on amiet's theory: effects of wind shear and atmospheric turbulence. *Acta Acustica united with Acustica*, 102:626–639, 2016.

[2] E. M. Salomons. *Computational atmospheric acoustics*. Kluwer Academic Publishers, 2001.

[3] R. K. Amiet. Acoustic radiation from an airfoil in a turbulent stream. *Journal of Sound and Vibration*, 41(4): 407–420, 1975.

[4] W. Zhu, N. Heilskov, W. Shen, and J.: Sørensen. Modeling of aerodynamically generated noise from wind turbines. *Journal of Solar Energy Engineering*, 127:517–528, 2005.

[5] N. Troldborg, C. Bak, H. Aagaard Madsen, and W. R. Skrzypinski. DANAERO MW: Final report, 2013.

[6] S. A. L. Glegg, S. M. Baxter, and A. G. Glendinning. The prediction of broadband noise from wind turbines. *Journal of Sound and Vibration*, 118(2):217–239, 1987.

[7] H. A. Madsen, C. Bak, U. S. Paulsen, M. Gaunaa, N. N. Sørensen, P. Fuglsang, and L. Jensen. The DAN–AERO MW experiments. In *48th AIAA Aerospace Sciences Meeting*, number AIAA-2010-0645, 2010.

[8] International Standard. Wind turbines – part 1: Design requirements. IEC 61400–01, 2005.

[9] T. F. Brooks, D. S. Pope, and M. A. Marcolini. Airfoil self-noise and prediction. NASA, 1218, 1989.

[10] M. Roger and S. Moreau. Extensions and limitations of analytical airfoil broadband noise models. *International Journal of Aeroacoustics*, 9(3):273–305, 2010.

[11] International Standard. Wind turbines – part 11: Acoustic noise measurement techniques. IEC 61400–11, 2012.

[12] M. V. Lowson. Assessment and prediction of wind turbine noise. Flow Solutions Ltd, 1993. ETSU W/13/00284/REP.

[13] J. Counihan. Adiabatic atmospheric boundary layer: a reviewed and analysis of data from the period 1880-1972. *Atmospheric Environment*, 9:871–905, 1975.

[14] R. W. Paterson and R. K. Amiet. Acoustic pradiation and surface pressure characteristics of an airfoil due to incident turbulence. NASA, 1976.

[15] T. F. Geyer, E. Sarradj, and M. Hobracht. Noise generated by a leading edge in anisotropic turbulence. In *Inter–Noise*, 2016.

[16] A. Thacker, S. Loyer, and S. Aubrun. Comparison of turbulence length scales assessed with three measurement systems in increasingly complex turbulent flows. *Experimental Thermal and Fluid Science*, 34:638–645, 2010.

[17] R. L. Burden and J. D. Faires. *Numerical analysis*. Brooks / Cole, 2010.